Published in final edited form as:
Biochemistry. 2008 February 26; 47(8): 2547–2558. doi:10.1021/bi701467g.

Evidence for the Involvement of Acid/Base Chemistry in the Reaction Catalyzed by the Type II Isopentenyl Diphosphate/ Dimethylallyl Diphosphate Isomerase from *Staphylococcus aureus*[†]

Christopher J. Thibodeaux, **Steven O. Mansoorabadi**, **William Kittleman**, **Wei-chen Chang**, and **Hung-wen Liu**[*]
Division of Medicinal Chemistry, College of Pharmacy, Department of Chemistry and Biochemistry, and Institute of Cellular and Molecular Biology, University of Texas at Austin, 1 University Station A1935, Austin, Texas 78712

Abstract

The type II isopentenyl diphosphate/dimethylallyl diphosphate isomerase (IDI-2) is a flavin mononucleotide (FMN)-dependent enzyme that catalyzes the reversible isomerization of isopentenyl pyrophosphate (IPP) to dimethylallyl pyrophosphate (DMAPP), a reaction with no net change in redox state of the coenzyme or substrate. Here, UV-vis spectral analysis of the IDI-2 reaction revealed the accumulation of a reduced neutral dihydroflavin intermediate when the reduced enzyme was incubated with IPP or DMAPP. When IDI-2 was reconstituted with 1-deazaFMN and 5-deazaFMN, similar reduced neutral forms of the deazaflavin analogues were observed in the presence of IPP. Single turnover stopped-flow absorbance experiments indicated that this flavin intermediate formed and decayed at kinetically competent rates in the pre-steady-state and, thus, most likely represents a true intermediate in the catalytic cycle. UV-vis spectra of the reaction mixtures reveal trace amounts of a neutral semiquinone, but evidence for the presence of IPP-based radicals could not be obtained by EPR spectroscopy. Rapid-mix chemical quench experiments show no burst in DMAPP formation, suggesting that the rate determining step in the forward direction (IPP to DMAPP) occurs prior to DMAPP formation. A solvent deuterium kinetic isotope effect ($^{D_2O}V_{max}$ = 1.5) was measured on v_o in steady-state kinetic experiments at saturating substrate concentrations. A substrate deuterium kinetic isotope effect was also measured on the initital velocity ($^{D}V_{max}$ = 1.8) and on the decay rate of the flavin intermediate ($^{D}k_s$ = 2.3) in single-turnover stopped-flow experiments using (*R*)-[2-^{2}H]-IPP. Taken together, these data suggest that the C2–H bond of IPP is cleaved in the rate determining step and that general acid/base catalysis may be involved during turnover. Possible mechanisms for the IDI-2 catalyzed reaction are presented and discussed in terms of the available X-ray crystal structures.

Isoprenoids comprise a large and ubiquitous class of metabolites that participate in numerous physiological processes (1–4). All isoprenoids are derived initially from the condensation of two isoprene units, isopentenyl pyrophosphate (IPP, **1**)1 and dimethylallyl pyrophosphate (DMAPP, **2**). Two biosynthetic pathways for the production of IPP and DMAPP are known, the mevalonate (MVA) pathway found in animals, fungi, and archaebacteria, and the non-mevalonate or methyl erythritol phosphate (MEP) pathway

[†]This work was supported in part by a Welch Foundation Grant (F-1511), a National Institutes of Health Grant (GM40541), and a National Institutes of Health Fellowship (GM082085) awarded to S.O.M.

[*]Corresponding author. Tel.: (512) 232-7811; fax: (512) 471-2746; h.w.liu@mail.utexas.edu.

found in most eubacteria, green algae, and the chloroplasts of higher plants (1, 5, 6). In the MVA pathway, DMAPP must be generated from IPP by an isopentenyl diphophate/dimethylallyl diphosphate isomerase (IDI, Scheme 1) (1). In the MEP pathway, both IPP and DMAPP are coproduced from 4-hydroxy-3-methyl-2-butenyl diphosphate in the same enzymatic reaction (catalyzed by IspH). However, most of the organisms that utilize the MEP pathway still contain IDI, presumably to regulate the cytosolic pools of these two essential isoprenoid building blocks (5–7).

Two types of structurally unrelated IDIs, which likely operate by distinct chemical mechanisms, have been identified in nature. The type I IDI (or IDI-1), which has been extensively studied, uses divalent metal ions (Mg^{2+} and Zn^{2+}) to elicit an acid/base mediated 1,3-antarafacial proton addition/elimination reaction through a 3° carbocation intermediate (8–12). The type II IDI (IDI-2), which was discovered more recently, requires flavin mononucleotide (FMN), a reduced nicotinamide adenine dinucleotide cofactor (either NADH or NADPH), and divalent metal ions (Mg^{2+}) for catalysis (13). Since its initial isolation from *Streptomyces* sp. CL190, IDI-2 enzymes have been found in many eubacteria and archaebacteria as part of either the MVA or the MEP biosynthetic pathways (13–15). Subsequent biochemical and structural characterization of IDI-2 (13, 15–22) has revealed that the IDI-2-FMN_{ox} complex is reduced with stoichiometric amounts of NAD(P)H via stereospecific transfer of the pro-*S* hydride and that the resultant IDI-2-FMN_{red} is capable of performing multiple turnovers (21). Recent redox titrations of IDI-2 from *Staphylococcus aureus* and *Thermus thermophilus* in the presence and absence of IPP (**1**) have shown that the apoenzyme thermodynamically stabilizes the neutral flavin semiquinone in the presence of IPP (21, 22). It was also found that the apoenzyme reconstituted with 5-deazaFMN is inactive, while 1-deazaFMN supports catalysis (19, 21). These data suggest that the flavin coenzyme is not simply required to maintain the active site structure, which has been proposed (17); rather, it plays an active role in the chemical transformation of IPP (**1**) to DMAPP (**2**). Cumulatively, these results are consistent with a mechanism involving a cryptic redox cycle (23), where a single electron is transferred from FMN_{red} to IPP (**1**) to generate a semiquinone and a substrate radical (**5** and **6**, respectively, Scheme 2) (19, 21). Substrate deprotonation and single electron transfer back to FMN_{sem} completes the isomerization and regenerates FMN_{red} for another round of catalysis. However, a recent study by Johnston et al. using radical clock mechanistic probes has called this single electron transfer mechanism into question (24).

Despite these initial studies, mechanistic information for IDI-2 is still relatively sparse. Although the neutral FMN_{sem} (**5**) has been observed in redox titration and photoreduction experiments (21, 22), the catalytic relevance of FMN_{sem} during turnover has not been established. Poulter and co-workers have recently shown that the semiquinone does not accumulate to significant levels in the steady state (22). Furthermore, they suggested that the enzyme-bound FMN intermediate that forms during the normal reaction is consistent with a neutral reduced dihydroflavin (**4**, Scheme 2). Although the steady-state kinetic parameters have been reported for a few IDI-2 enzymes (13, 15, 18, 21, 22, 25), the nature of the rate limiting step(s) in the catalytic mechanism is unknown. In this paper, we report the investigation of the FMN intermediate formed during the catalysis of *S. aureus* IDI-2 using UV–vis and EPR spectroscopies. The catalytic competence of the FMN intermediate was

[1]Abbreviations: IDI, isopentenyl diphosphate/dimethylallyl diphosphate isomerase; IDI-1, type I IDI; IDI-2, type II IDI; IPP, isopentenyl pyrophosphate; DMAPP, dimethylallyl pyrophosphate; FMN, flavin mononucleotide; 1-deazaFMN, 1-carba-1-deazariboflavin-5′-phosphate; 5-deazaFMN, 5-carba-5-deazariboflavin-5′-phosphate; FMN_{ox}, oxidized FMN; FMN_{red}, reduced FMN; FMN_{sem}, FMN semiquinone; EPR, electron paramagnetic resonance; KIE, kinetic isotope effect; MEP, methyl erythritol phosphate; NADPH, nicotinamide adenine dinucleotide phosphate (reduced form); TAPS, *N*-tris(hydroxymethyl)methyl-3-aminopropanesulfonic acid; HEPES, *N*-[2-hydroxy]piperizine-*N*′-[2-ethanesulfonic acid]; DTT, dithiothreitol; CS, chorismate synthase; EIPP, 3,4-epoxy-3-methylbutyl diphosphate.

probed by stopped-flow spectrophotometry under both single- and multiple-turnover conditions, and the possible presence of flavin and substrate-derived radical intermediates was studied by EPR spectroscopy under anaerobic conditions. Rapid-mix chemical quench experiments and steady-state kinetic isotope effect studies were also performed to investigate the rate limiting catalytic step(s). Together, these data provide much needed insight into the mechanism of this intriguing flavoprotein. Several reaction mechanisms are proposed and are discussed in terms of the available IDI-2 crystal structures.

EXPERIMENTAL PROCEDURES

General

The pQES plasmid containing the *idi2* gene from *S. aureus* was a generous gift from Prof. Haruo Seto (Tokyo University of Agriculture) and was transformed into *Escherichia coli* M15[pREP4] (Qiagen, Valencia, CA) for gene expression. Recombinant IDI-2 was overproduced as an N-terminal His_6 fusion protein and purified as described previously (21). IDI-2 stock concentrations were determined by the Bradford assay (26) and by the extinction coefficient at 280 nm (34 400 M^{-1} cm^{-1}) determined by quantitative amino acid analysis. IPP (27), DMAPP (27), (*R*)-[2-^{2}H]-IPP (28), 1-deazaFMN (29), and 5-deazaFMN (29) were synthesized and purified according to established protocols. Flavin mononucleotide (FMN) (98%), reduced nicotinamide adenine dinucleotide phosphate (NADPH), and *N*-tris(hydroxymethyl) methyl-3-aminopropane-sulfonic acid (TAPS, 99.5%) were purchased from Sigma-Aldrich (St. Louis, MO). Sodium dithionite ($Na_2S_2O_4$, 85%) and petroleum ether (bp 60–95 °C) were acquired from Acros Organics (Geel, Belgium). [1-^{14}C]-IPP (55 mCi/mmol) was a product of American Radiolabeled Chemicals, Inc. (St. Louis, MO). *N*-[2-Hydroxy]piperizine-*N*′-[2-ethanesulfonic acid] (HEPES, 99%) was purchased from USB Corporation (Cleveland, OH), and dithiothreitol (DTT, molecular biology grade) and $MgCl_2$ were purchased from Fisher Scientific (Fair Lawn, NJ).

Preparation of Anaerobic Buffers

All buffers and reaction components used for anaerobic experiments were degassed using a Schlenk line and oxygen-free argon. Small volumes (~150 μL) were made anaerobic by bubbling argon into the solution for 20–30 min, and large volumes (>1 mL) were degassed for 2 h. IDI-2 was made anaerobic by alternating cycles of vacuum (5 s) and argon purging (20 s). Following degassing, all anaerobic components were immediately transferred to a Coy Laboratories anaerobic chamber (Grass Lakes, MI) containing an atmosphere of 95% N_2 and 5% H_2 ($O_2 \leq 5$ ppm).

UV–vis Spectroscopy of Reaction Mixtures under Anaerobic Conditions

All buffers and reaction components were degassed as described previously. A typical reaction mixture (500 μL) contained 80 μM IDI-2, 200 μM FMN_{ox}, 5 mM $MgCl_2$, and 1 mM DTT in 100 mM HEPES, pH 7.0. E•FMN_{ox} was reduced either chemically with 10 mM NADPH or $Na_2S_2O_4$ or by photoreduction using short periods of illumination (15 s) from a Kodak Carousel Slide Projector. Generally, a total illumination time of 3–5 min was sufficient for complete photoreduction of the enzyme-bound flavin. To determine the flavin intermediate absorption spectrum, a saturating concentration of IPP or DMAPP (2 mM) was added to the reaction under anaerobic conditions. Spectra were recorded with a diode array spectrophotometer (Agilent Technologies, Inc., Kenner, LA) at 25 °C. Following data acquisition, the spectra were normalized at 900 nm.

UV–vis Spectra of Enzyme-Bound Flavin Analogues

Anaerobic UV–vis spectra were also recorded for enzyme-bound 1-deazaFMN and 5-deazaFMN in the presence and absence of substrate in 50 mM potassium phosphate buffer (pH 7.0 and 25 °C). For 5-deazaFMN, 80 μM oxidized coenzyme (K_d = 16 μM) (21) was incubated with 100 μM IDI-2, and the reaction was photoreduced as described previously. For 1-deazaFMN, coenzyme and enzyme concentrations were slightly scaled up to 150 and 200 μM, respectively, to account for the weaker binding of 1-deazaFMN$_{ox}$ (K_d = 97 μM) (21), and the coenzyme was reduced with 50 mM $Na_2S_2O_4$. IPP (1 mM) was then added to the reduced enzymes to generate the intermediate spectrum. The UV–vis spectra of IDI-2 reconstituted with the flavin analogues were corrected for the presence of native FMN (which copurifies with IDI-2 at about 10% of the total enzyme concentration).

Stopped-Flow Assays

To verify the catalytic competence of the flavin intermediate observed in anaerobic assay mixtures, stopped-flow kinetic analyses were performed. Multiple-turnover stopped-flow reactions contained 68 μM IDI-2, 2 mM substrate (IPP, DMAPP, or (*R*)-[2-^{2}H]-IPP), 200 μM FMN, 10 mM $Na_2S_2O_4$, 5 mM $MgCl_2$, and 1 mM DTT in 100 mM HEPES buffer (pH 7.0 and 37 °C). Here, one syringe contained 136 μM IDI-2, and the other syringe contained 4 mM substrate. Both syringes contained 200 μM FMN, 10 mM $Na_2S_2O_4$, 5 mM $MgCl_2$, and 1 mM DTT. The reaction was monitored with a diode array detector, and the observed rate of flavin intermediate formation was determined by fitting the time dependence of the absorbance changes at 435 nm to a single-exponential equation (eq 1) using GraFit 5.

$$A_{435}=A(1-e^{-k_{obs}t})+C \quad (1)$$

Here, k_{obs} is the observed first-order rate of flavin intermediate formation, A is the total amplitude change of the absorbance signal at 435 nm, and C is the initial absorbance signal. For single-turnover stopped-flow experiments, the final concentrations after mixing were 69 μM IDI-2, 50 μM IPP or (*R*)-[2-^{2}H]-IPP, 200 μM FMN, 10 mM $Na_2S_2O_4$, 5 mM $MgCl_2$, and 1 mM DTT in 100 mM potassium phosphate buffer (pH 7.0 and 37 °C). The absorbance changes were monitored with a diode array attachment over 5 s intervals, and the time courses were fit to a double-exponential equation (eq 2)

$$A_{435}=A_f(1-e^{-k_f t})+A_s(1-e^{-k_s t})+C \quad (2)$$

where A_f and k_f are the amplitude and observed rate of the fast phase, A_s and k_s are the amplitude and rate of the slow phase, and C is the A_{435} value at t = 0. A total of eight injections was performed with each substrate (either IPP or (*R*)-[2-^{2}H]-IPP), and the amplitudes and rates reported are the averaged values.

EPR Analysis of Anaerobic Reaction Mixtures

To detect trace amounts of flavin semiquinone and/or substrate radicals that may be forming during turnover, anaerobic reaction mixtures were prepared for EPR analysis. The reaction conditions and reagent concentrations were identical to those used to generate the UV–vis spectra. E•FMN$_{ox}$ was reduced with either 10 mM NADPH, 10 mM $Na_2S_2O_4$, or by photoreduction. Following the addition of 2 mM IPP, the mixtures were transferred to an EPR tube, were allowed to react for 2 min, and were then flash frozen in isopentane cooled in a dewar of liquid nitrogen. In a separate reaction, IPP was pre-incubated with E•FMN$_{ox}$, and the E•FMN$_{ox}$•IPP complex was photoreduced for 2 min prior to freezing. The EPR samples were stored in liquid nitrogen until they were analyzed. X-band EPR spectra were

recorded at 100 K on a Bruker EMX spectrometer. Spin concentrations were determined by double integration using the WinEPR (version 2.11) software package and comparison to a standard mixture containing 1 mM $CuSO_4$, 10 mM EDTA, and 100 mM $NaClO_4$.

Rapid Chemical Quench Experiments

To analyze the rate of DMAPP formation in pre-steady-state time regimes, a rapid chemical quench experiment was performed with a KinTek RFQ-3 rapid-quench flow system. The reactions were carried out at 37 °C with 20 μM IDI-2, 100 μM FMN, 100 mM dithionite, 520 μM [1-^{14}C]-IPP (1.92 μCi/μmol), 5 mM $MgCl_2$, and 1 mM DTT in 100 mM HEPES, pH 7.0 (enzyme and IPP were kept in separate syringes prior to mixing). The reactants were allowed to mix for variable lengths of time (from 3 ms to 1 s) prior to quenching with a solution of HCl/MeOH (25%). Each time point was acquired in duplicate, and the transfer of the ^{14}C radiolabel from IPP to DMAPP at each quenched time point was determined using a modified Satterwhite activity assay (13). Each quenched sample was immediately incubated at 37 °C for 10 min to allow conversion of the acid-labile DMAPP product into a mixture of extractable alcohols and methyl ethers. These compounds were then separated from unreacted [1-^{14}C]-IPP by extraction with 1 mL of petroleum ether. A 300 μL portion of the organic fraction was added to 6 mL of nonaqueous scintillation fluid (Amersham Biosciences) and analyzed by a Beckman Coulter LS 6500 multi-purpose scintillation counter. The specific activity of [1-^{14}C]-IPP in the reaction was used, along with the radioactivity of the organic fraction, to calculate the concentration of DMAPP present in each quenched sample. The DMAPP concentrations were then normalized by the total enzyme concentration, plotted versus time, and fitted using linear regression to determine the pre-steady-state rate of DMAPP formation.

In Situ NMR Assay for Initial Velocity Determination

To obtain an accurate measurement for $^{D}V_{max}$ using (*R*)-[2-^{2}H]-IPP, we employed an in situ NMR assay similar to that reported by Laupitz et al. (15) to directly monitor the formation of DMAPP from IPP or (*R*)-[2-^{2}H]-IPP under initial velocity conditions. The reaction mixtures (660 μL) contained 90 nM IDI-2, 10 mM IPP (or (*R*)-[2-^{2}H]-IPP), 10 μM FMN, 10 mM sodium dithionite, 2.0 mM sodium acetate (internal standard), 1 mM DTT, 5 mM $MgCl_2$, and 9% (v/v) D_2O (as a reference) in 100 mM potassium phosphate buffer (pH 7.0 and 37 °C). After shimming and initial peak integration, enzyme was added to the NMR tube, and the appearance of the (*Z*)-methyl proton resonance of DMAPP (δ = 1.66 ppm) (13, 15, 28) was followed over 120 min using a Varian Unity 500 MHz NMR spectrometer. The spectra at each individual time point were acquired over a 220 s interval, and a 180 s delay time was used between successive data acquisition periods. The concentration of DMAPP at each time point was calculated from the integrated peak areas of the resonance at δ = 1.66 ppm by normalizing to the peak area of the 2 mM acetate internal standard at δ = 1.84 ppm.

Solvent Kinetic Isotope Effects

The initial velocity of DMAPP formation was measured over the pL range of 7.0–8.5 (pL = pH or pD; pD = pH meter reading + 0.4). A stock buffer solution containing FMN, DTT, and $MgCl_2$ in HEPES (pL 7.0 and 7.5) or TAPS (pL 8.0 and 8.5) was made in either H_2O or D_2O and then adjusted to the desired pL value with 10 M NaOH. For the reactions carried out in D_2O, the final mole fraction of protium (derived from buffer components, enzyme stock solution and NaOH) was less than 5% at each pL. After degassing buffers and component solutions, the reagents were transferred to the glove box. The final reaction mixtures contained 56.3 nM IDI-2, 10 μM FMN, 10 mM dithionite, 5 mM $MgCl_2$, 1 mM DTT, and 269 μM IPP (11 μCi/μmol). All components (except substrate) were pre-incubated at 37 °C for 10 min prior to the addition of IPP to initiate the reaction. At 0.5, 2.5, 4.5, 6.5, and 8.5 min intervals, 50 μL aliquots of the reaction were quenched with 200 μL of

25% HCl/MeOH. The subsequent workup, extraction, and scintillation counting conditions were identical to those described for the rapid-quench experiments. The initial velocities at 269 μM IPP were measured in triplicate, and the solvent KIE was calculated from the averaged values of $^{D_2O}V_{max}$ and $^{H_2O}V_{max}$ at each pL.

RESULTS

The UV–vis spectra of the IDI-2-bound FMN in its various oxidation states are shown in Figure 1A. The oxidized coenzyme (E•FMN_{ox}) was characterized by absorbance maxima at 374 and 452 nm, while the photoreduced coenzyme (E•FMN_{red}) has a λ_{max} value at 345 nm and a large shoulder at 390 nm, suggesting that at pH 7.0, E•FMN_{red} is predominantly in the anionic form (30). The addition of 2 mM IPP to this photoreduced E•FMN_{red} sample led to new peaks at 324 and 435 nm. Although absorbance changes <400 nm cannot be accurately measured in NADPH- and dithionite reduced preparations, A_{435} also increases in incubations with these reductants and 2 mM IPP, DMAPP, or (*R*)-[2-^{2}H]-IPP, suggesting that a similar flavin intermediate forms regardless of the reduction method or reaction direction (the dithionite reduced reaction spectra are shown in Figure 1B). The λ_{max} value at 435 nm is unusual for flavoproteins but is most consistent with a neutral reduced FMN (as suggested previously for IDI-2 (22, 31)), which has been observed to have a λ_{max} value anywhere from 390 to 450 nm, depending on the hydrophobicity and rigidity of the active site environment (32–35). Consistent with previous photoreduction studies (22), a neutral semiquinone (E•FMN_{sem}) could be generated under anaerobic conditions if 2 mM IPP was pre-incubated with E•FMN_{ox} prior to a 2 min photoreduction. On the basis of the ε_{583} (3300 M^{-1} cm^{-1}) value determined previously for the *S. aureus* IDI-2-bound FMN_{sem} (21), the concentration of FMN_{sem} in this photoreduced sample is estimated to be 25 μM (or about 31% of the total E•FMN concentration).

Similar reaction mixtures were prepared with 5-deazaFMN and 1-deazaFMN (Figure 2). Oxidized E•5-deazaFMN (λ_{max} values at 341 and 401 nm) was easily photoreduced to a state with μ_{max} = 320 nm, which is typical of the anionic reduced coenzyme (36). When IPP was added, a slight red shift to 326 nm was observed for this peak, suggesting that the coenzyme becomes protonated in the presence of IPP (33, 36). Oxidized E•1-deazaFMN (μ_{max} = 538 nm) could not be photoreduced, but reduction with 50 mM sodium dithionite yielded the anionic 1-deazaFMN_{red}, which has a rather featureless absorbance spectrum >400 nm (37). The addition of IPP led to the formation of a species with μ_{max} = 436 nm, also indicative of a neutral 1-deazaFMN_{red} (37, 38). Thus, with all three flavins, the shifts in the UV–vis spectra of the reduced coenzymes in the presence of IPP appear to be consistent with the formation of the neutral reduced coenzyme, which may form via protonation of the corresponding anionic reduced flavin at the N1–C2═O2′ (or C1–C2═O2′ for 1-deazaFMN) locus by an active site residue upon formation of the Michaelis complexes.

To verify the catalytic competence of the observed flavin intermediate, the dithionite reduced enzyme was analyzed using stopped-flow spectrophotometry under single- and multiple-turnover conditions. For multiple-turnover reactions, the enzyme was mixed with a saturating concentration (2 mM) of IPP, (*R*)-[2-^{2}H]-IPP, or DMAPP, and the pre-steady state changes in the absorbance spectrum were recorded with diode array detection over a 400 ms time interval. The time-dependent absorbance changes for all three reactions at 435 nm are shown in Figure 3A. As can be seen for the IPP reaction, there is a rapid accumulation (k_{obs} = 52 ± 0.9 s^{-1}) of the flavin intermediate in the pre-steady state, which is clearly faster than k_{cat} (1.9 s^{-1}). A similar flavin intermediate also forms quickly in the reverse direction (DMAPP to IPP) with k_{obs} = 14.8 ± 0.4 s^{-1}. The pre-steady-state kinetics with (*R*)-[2-^{2}H]-IPP as the substrate were similar to those of IPP, except that k_{obs} was smaller (40.9 ± 0.5 s^{-1}), and the amplitude of the absorbance change was slightly larger (Figure 3A). This

slightly larger amplitude change may indicate that (*R*)-[2-^{2}H]-IPP binding is tighter or that turnover is slower, such that a larger fraction of the E•FMN_{red}•IPP Michaelis complex accumulates in the pre-steady state.

The stopped-flow diode array reactions were also carried out under single-turnover conditions with 50 μM IPP or (*R*)-[2-^{2}H]-IPP and 69 μM E•FMN_{red}. In these reactions, the changes in A_{435} were biphasic and were characterized by a rapid increase in A_{435}, followed by a slower decrease (Figure 4). The time courses were fit to a double-exponential equation (eq 2) to extract values for the amplitudes and the apparent first-order rate constants of both phases. As shown in Figure 4, the flavin intermediate formed at apparent first-order rates (k_f) of 34 ± 2.4 s^{-1} for IPP and 23 ± 0.9 s^{-1} for (*R*)-[2-^{2}H]-IPP, yielding ^Dk_f = 1.5 ± 0.1. Interestingly, the decay rate of the flavin intermediate in the slow phase (k_s = 2.1 ± 0.4 s^{-1} for IPP and 0.9 ± 0.05 s^{-1} for (*R*)-[2-^{2}H]-IPP) gives a ^Dk_s value of 2.3 ± 0.5, which is very similar to the $^DV_{max}$ value on DMAPP formation determined by the NMR assay (vide infra). This apparent KIE value on k_s is consistent with the inclusion of the cleavage of the C2–H bond in the slow phase. The nonequivalent magnitudes of the fast and slow phase amplitudes for both reactions suggest that an internal equilibrium is established in which anionic (E•$FMNH^-$, E•$FMNH^-$•IPP, and E•$FMNH^-$•DMAPP) and neutral (E•$FMNH_2$, E•$FMNH_2$•IPP, and E•$FMNH_2$•DMAPP) reduced flavin-containing enzyme forms are present. No additional flavin intermediates (including semiquinones, λ_{max} = 583 nm) were detected in single- or multiple-turnover stopped-flow experiments. These data suggest that the $FMNH_2$ intermediate is kinetically competent and is likely on the catalytic pathway.

Although the neutral FMN_{sem} forms in photoreduction and redox titration experiments when IPP is mixed with the catalytically inactive E•FMN_{ox} (21, 22), it did not accumulate to significant levels when IPP was mixed with the catalytically active E•FMN_{red} in stopped-flow experiments. However, there did appear to be very small differences in the A_{583} values between the blank and the reaction mixtures (see Figure 1B). To investigate the potential existence and relevance of a semiquinone during catalysis, and to look for substrate-derived radical species, we recorded EPR spectra of various reaction mixtures at 100 K (Figure 5A). In dithionite-, NADPH-, and photoreduced mixtures, E•FMN_{sem} was detectable, but its concentration represented <1% of the total enzyme concentration. In contrast, when E•FMN_{ox} was pre-mixed with IPP and then photoreduced for 2 min, large quantities of E•FMN_{sem} (~37% of the total enzyme concentration) were generated (Figure 5B). The *g*-values (*g* = 2.00) and line-widths (21 G) of these signals are consistent with a neutral FMN_{sem} (39). The absence of any other observable radical signals in the EPR spectrum, and the lack of zero-field splitting in the FMN_{sem} signal, indicates that the flavin semiquinone that accumulates in the reaction mixtures is not coupled to an IPP-based radical in the IDI-2 active site. These observations strongly suggest that the observed flavin semiquinone is not catalytically relevant. These results for the *S. aureus* enzyme are consistent with the EPR data recently reported by Rothman et al. for the *T. thermophilus* IDI-2 enzyme (22).

To determine the position of the rate determining step(s) relative to DMAPP formation in the reaction course, we performed rapid-quench experiments. If the rate determining step occurs after DMAPP formation, then DMAPP is expected to accumulate at the active site in the pre-steady state, and a burst of DMAPP formation will be visible. However, for the IDI-2 catalyzed reaction, the formation of DMAPP with a saturating IPP concentration (520 μM) was linear, and no burst was observed (Figure 6). Although the derivitized DMAPP ^{14}C signals at early time points are significantly above zero (*y*-intercept = 0.04 ± 0.01 or about 4% of the total enzyme concentration), they are barely above the instrument noise level. Thus, this small *y*-intercept probably does not reflect a true burst of product formation. The rate of DMAPP formation determined from the burst experiment (1.4 ± 0.01 s^{-1}) is similar to the steady-state k_{cat} values measured previously for the *S. aureus* IDI-2 (13,

21). These data are consistent with the rate limiting step occurring prior to DMAPP formation and after the rapid accumulation of the flavin intermediate at 52 ± 0.9 s^{-1} (Figure 3A). Thus, chemistry is likely rate limiting in the forward reaction (IPP to DMAPP).

To more closely probe the rate limiting step(s), we performed kinetic isotope effect studies using deuterated substrate ((*R*)-[2-^{2}H]-IPP) and solvent (D_2O). We have previously shown that the *pro-R* proton at the C2 of IPP is removed during turnover (28). To determine whether cleavage of this C2–H bond contributes to the steady-state rate limitation, in situ ^{1}H NMR assays were carried out with both unlabeled IPP and (*R*)-[2-^{2}H]-IPP. In this experiment, the appearance of the (*E*)- and (*Z*)-methyl signals of DMAPP (δ = 1.70 and 1.66 ppm, respectively) and the disappearance of the C4′ methyl peak of IPP (δ = 1.72 ppm) were monitored (Figure 7A). Following the conversion of the integrated peak areas into concentration units (based on comparison with an acetate internal standard), it is clear that DMAPP formation from both substrates is linear over the entire time course (Figure 7B). The initial velocity of DMAPP formation for the IPP and (*R*)-[2-^{2}H]-IPP reactions were 0.170 ± 0.001 μM s^{-1} (k_{cat} = 1.8 ± 0.01 s^{-1}) and 0.093 ± 0.002 μM s^{-1} (k_{cat} = 1.0 ± 0.02 s^{-1}), respectively (Figure 7B), which corresponds to $^{D}V_{max}$ = 1.8 ± 0.04. The magnitude of $^{D}V_{max}$ clearly indicates that the C2–H bond cleavage is at least partially rate limiting in the forward direction.

To assess as to whether solvent exchangeable protons are transferred in the rate determining step(s), we also performed steady-state kinetic assays in H_2O and D_2O over the pL range of 7.0–8.5. For this experiment, the initial velocity (v_o) at a single IPP concentration of 269 μM was measured in triplicate at each pL value. Since this IPP concentration is ~10 times the K_m of IPP (28 μM), the initial velocities measured should be roughly equal to V_{max} under these conditions. Our data reveal a normal solvent kinetic isotope effect ($^{D2O}V_{max}$) across the pL range tested (Figure 8). In D_2O, V_{max} increases from pL 7.0 to 8.0, while in H_2O, it is relatively independent across the pL range. The $^{D2O}V_{max}$ value was calculated to be 1.4 ± 0.08 at pL 8.0 (which appears to be the pL-independent region in both solvents). These data suggest that solvent exchangeable protons are transferred in the rate determining step. Together, the kinetic data reported herein suggest that the rate limiting step in the IDI-2 catalyzed reaction likely involves general acid/base catalysis after the fast accumulation of the neutral FMN_{red}.

DISCUSSION

The studies reported herein were aimed at characterizing the flavin intermediate generated in the IDI-2 reactions with FMN or flavin analogues using transient kinetic methods and UV–vis and EPR spectroscopy. Our experimental results support the intermediacy of a neutral reduced flavin ($FMNH_2$), which forms upon IPP or DMAPP binding to form the Michaelis complex. Similar observations were also made by Rothman et al. (22). The spectral changes for the reduced, enzyme-bound 1-deaza and 5-deazaFMN analogues in the presence of IPP are also consistent with the accumulation of their neutral reduced forms. The protonation in the N1/C1–C2═O2′ region of all three coenzymes may be mediated by Lys186 or His149 (*S. aureus* numbering), both of which are absolutely conserved among IDI-2 enzymes (15–17, 20). Previously, we have suggested that IPP binding may induce a conformational change that results in a K_m value for reduced FMN (200 nM) that is 70-fold lower than the K_d (14 μM) value for binding of the reduced FMN to IDI-2 in the absence of IPP (21). This conformational change induced by substrate binding may help to position the acid for the protonation of the anionic FMN_{red} in the Michaelis complex. Preliminary studies have also shown that the spectra of the flavin intermediate at pH 7.0 and 8.0 are very similar, while at pH 9.0, a larger fraction of FMN_{red} remains anionic in the presence of IPP. These data suggest that the active site group responsible for FMN protonation may have a pK_a value

near 9.0 and is thus more likely Lys186. Rothman et al. also observed a similar trend and suggested the existence of a general acid with a pK_a value of about 8.5 for the *T. thermophilus* enzyme (22).

The catalytic competence of the neutral reduced flavin intermediate was verified in this work by both multiple- and single-turnover stopped-flow experiments (Figures 3A and 4, respectively). During the single-turnover stopped-flow experiments, the neutral reduced $FMNH_2$ was observed to accumulate in a fast phase upon IPP binding, before decaying to an equilibrium level in a kinetically competent slow phase. No additional intermediates (such as a flavin semiquinone) were observed. Correspondingly, a flavin semiquinone/substrate radical pair could not be detected in steady-state reaction mixtures by EPR spectroscopy, which revealed that only about 1% of the total enzyme contained a magnetically isolated semiquinone (Figure 5). From the present data, it appears that this neutral semiquinone, which has been observed during photoreduction and redox titration experiments (21, 22), may not be catalytically relevant. More likely, it seems that IPP binding in the active site alters the environment around the flavin coenzyme such that the redox potential of the $E{\bullet}FMN_{ox}/E{\bullet}FMN_{sem}$ couple is elevated relative to the $E{\bullet}FMN_{sem}/E{\bullet}FMN_{red}$ couple. This enables the one-electron reduction of $E{\bullet}FMN_{ox}{\bullet}IPP$ through a stable semiquinone intermediate. The thermodynamic stabilization of the neutral semiquinone in these previous studies has been difficult to reconcile with the apparent lack of a similar species in catalytically competent reaction mixtures. If a kinetically relevant substrate radical is indeed forming along with a neutral flavin semiquinone, its steady-state concentration must be exceedingly low.

To gain an understanding of the rate limiting step(s) in the overall reaction, we performed rapid-mix chemical quench (Figure 6), single-turnover stopped flow (Figure 4), and kinetic isotope effect experiments (Figures 7 and 8). The rapid-mix chemical quench experiment clearly showed no burst in DMAPP formation. Thus, the rate limiting step in the forward reaction (IPP to DMAPP) must occur prior to the formation of DMAPP and after the rapid accumulation of the neutral FMN_{red} in the active site. Furthermore, the rate determining step most likely involves isomerization chemistry. This assertion is supported by the measurement of both a solvent deuterium KIE ($^{D_2O}V_{max}$ = 1.5, Figure 8) and a 1° substrate deuterium KIE ($^{D}V_{max}$ = 1.8, Figure 7) using the deuterated substrate (*R*)-[2-^{2}H]-IPP. A significant 1° deuterium KIE was also observed on the decay rate of the neutral reduced flavin intermediate ($^{D}k_s$ = 2.3, Figure 4) in single-turnover stopped-flow experiments with (*R*)-[2-^{2}H]-IPP. While $^{D}k_s$ and $^{D}V_{max}$ clearly demonstrate that cleavage of the IPP C2–H bond is partially rate limiting and is kinetically linked to the decay of the flavin intermediate, the origin of $^{D_2O}V_{max}$ is less obvious but may arise from protonation of the IPP double bond by an active site acid. This protonation event would help to lower the pK_a value of C2–H, which is otherwise not acidic. A general acid protonation mechanism has recently been proposed to be responsible for the covalent modification (and inactivation) of the IDI-2-bound reduced flavin by two separate epoxide inhibitors (23, 39). These data are discussed in more detail below.

A central, unresolved question in the IDI-2 catalyzed reaction is the exact role of the flavin coenzyme. Kinetic experiments have shown that the apoenzyme reconstituted with 5-deazaFMN is inactive (19, 21), while the enzyme reconstituted with 1-deazaFMN is active (21). The inactivity of 5-deazaFMN and the lack of transient formation of a fully oxidized FMN intermediate in the stopped-flow studies are inconsistent with a mechanism involving transient donation of a hydride equivalent from reduced FMN to IPP to generate a 3-methylbutyl intermediate (23). Instead, these early observations, along with the thermodynamic stabilization of the neutral FMN_{sem} in the presence of IPP (21, 22), appeared to suggest a mechanism involving single electron transfer chemistry (21, 23). In

the single electron transfer mechanism (Scheme 2), the reaction is initiated by IPP binding and the formation of the neutral FMN_{red} (**4**). This is followed by the deprotonation of the flavin N1 and protonation at C4 of IPP (or at *C*2 of DMAPP in the reverse direction), triggering the subsequent electron transfer from the anionic FMN_{red} to IPP (**1**). Generation of the neutral FMN_{sem}/IPP radical pair (**5** and **6**) should lower the pK_a of the *pro-R C*2 proton of **6**, allowing its removal by a general base and concomitant electron transfer back to the FMN_{sem} to complete the cryptic redox cycle.

However, the electron transfer mechanism is inconsistent with many lines of evidence gathered in more recent experiments, including the futile attempts to detect a substrate-based radical (22) and our inability to detect a catalytically competent FMN_{sem} in single-turnover stopped flow experiments. Furthermore, if an active site acid is capable of protonating IPP at C4, it is not clear why the flavin would need to transfer an electron to the 3° carbocation, as the *C*2–H (pK_a ~ −12 (40)) would already be sufficiently activated for abstraction. Also, unless electron transfer in the IDI-2 active site is gated by proton transfer, it is not obvious why the k_{cat} measured with 1-deazaFMN$_{red}$ (whose redox potential is substantially lower than FMN_{red}), is nearly identical to the k_{cat} measured with FMN_{red} (21). Unless the electron transfer occurs in the inverted Marcus region, the accumulation of the neutral FMN_{red} seems puzzling, since the anionic FMN_{red} is a better thermodynamic reductant than the protonated, neutral form. Finally, the inability to detect radical fragmentation products in incubations with a cyclopropane-containing, radical clock IPP substrate analogue strongly suggests that single electron transfer is not involved in the isomerization of the double bond of this substrate analogue (24).

As an alternative to the electron transfer mechanism, IDI-2 may catalyze the isomerization reaction solely by acid/base chemistry (mechanisms A–D, Scheme 3) in a manner similar to the IDI-1 catalyzed reaction (11). All of these mechanisms are based on the following assumptions: (i) Substrate binding leads to the rapid accumulation of the neutral reduced FMN (**4**) in both the forward and the reverse directions (as observed in the single- and multiple-turnover stopped flow studies), (ii) the rate limiting step occurs before DMAPP formation in the forward direction (as indicated by the rapid-quench studies), and (iii) the rate limiting step involves acid/base chemistry (as suggested by the KIE studies). For simplicity, the substrate binding steps and the conversion of $FMNH^-$ to $FMNH_2$ are not shown in Scheme 3. In one possible acid/base mechanism (Scheme 3A), the FMN coenzyme may play a role in the stabilization of a 3° carbocation intermediate (**7**) through cation–π interactions, similar to the function proposed for a conserved tryptophan residue (Trp161 in *E. coli*) in the IDI-1 enzyme. This mechanism, however, has a few loopholes. For example, it is not clear as to why 5-deazaFMN does not support catalysis, unless this cation–π interaction depends strongly on the N5 atom or a hydrogen bonding network maintained by the N5 atom. Also, it is not clear as to why the neutral form of the reduced coenzyme (**4**) accumulates upon the addition of substrate, as the anionic form should be better suited to stabilize a carbocation intermediate through electrostatic interactions.

If the flavin does not simply perform a structural or electrostatic stabilization role, then it could be acting directly as the active site acid (Scheme 3B), the active site base (Scheme 3C), or both (Scheme 3D) (22, 31). The acidic function may be fulfilled by the flavin N5-H group (Scheme 3B). This assignment could account for the accumulation of the neutral FMN_{red} upon substrate binding. The pK_a value of the N5 proton of neutral FMN_{red} is typically ~20 (41–43) but could be lowered not only by the protonation of N1 in the Michaelis complex but also by the donation of a hydrogen bond from an absolutely conserved threonine residue (Thr67 in *S. aureus*), which is 2.9 Å from N5 of FMN_{ox} in the *Bacillus subtilis* crystal structure (16). In the case of acyl-CoA dehydrogenases, a hydrogen bond donated from a conserved Thr to N5 of FAD_{ox} is believed to decrease the electron

density of the flavin ring system that, in turn, facilitates the formation of a charge transfer interaction between the substrate derived enolate and the electron deficient FAD_{ox} (44). In the case of IDI-2, the hydrogen bond from Thr67 to N5 may have a similar effect—to steal electron density from the flavin ring system, lowering the pK_a value of the N5 proton, and allowing its transfer to the double bond of IPP (or DMAPP), while a separate active site base deprotonates C2. Alternatively, the N5 atom could also act as a base, while a separate active site acid carries out the protonation (Scheme 3C). In this case, Thr67 may accept a hydrogen bond from the flavin, increasing the basicity of the N5 atom. Mechanisms involving the reduced flavin as both an acid and a base can also be envisioned. Previously, Rothman et al. have suggested that a zwitterionic 5,5-dihydro reduced flavin tautomer could be involved in IDI-2 catalysis based on the appearance of an absorption band at ~320 nm that forms upon IPP binding, which is similar to the absorption λ_{max} value reported for an N5-dimethylated reduced flavin (22). However, 1,5-dihydroflavin tautomers can also absorb in this region (32). It is also possible that the neutral reduced flavin that accumulates upon IPP binding is protonated at O4′ rather that at N1, giving the tautomer **10** (Scheme 3D). While not typically considered for FMN, protonation at this locus is known to occur in 1-deazaflavins (37). Tautomer **10** could protonate the IPP double bond to give a carbocation (**7**) and an anionic reduced flavin (**11**). A proton relay mediated by Thr67 (which is also within hydrogen bonding distance of O4′ in the *B. subtilis* structure) could serve to reprotonate O4′ and simultaneously activate N5 as a base to complete the isomerization. It is important to note that the 1-deazaFMN coenzyme is expected to be active in mechanisms where transient protonation/deprotonation of the flavin N5 position is required for turnover. On the other hand, reduced 5-deazaFMN, which lacks the lone electron pair at the C5 locus, would not be able to mediate these proton transfers.

For these acid/base mechanisms involving direct participation of the neutral FMN_{red}, IPP (or DMAPP) would have to bind in the vicinity of N5. Curiously, Eguchi and co-workers recently isolated an N5-alkyl adduct formed upon incubation of the reduced IDI-2 from *Methanocaldococcus jannaschii* with an epoxide analogue of IPP (3,4-epoxy-3-methylbutyl diphosphate, EIPP) (25). Using a separate epoxide analogue and the *T. thermophilus* enzyme, Poulter and co-workers isolated a similar inactivation adduct (24). Both groups concluded that an active site acid protonates the epoxide, leading to a carbocation that is trapped by the nucleophilic N5 atom of the reduced flavin. These results clearly indicate that both epoxide inhibitors bind near the flavin N5, which can accumulate sufficient electron density to serve as a nucleophile to form a covalent adduct with the epoxide compounds. As to whether the flavin is directly involved in epoxide protonation is unknown, but these inactivation studies provide tantalizing hints that the flavin may play an active role in the acid/base chemistry of the normal reaction. Unfortunately, little information on the identity of the putative acid/base groups can be gleaned from the available crystal structures, which were solved with the inactive FMN_{ox} bound in the active site in the absence of substrate (16, 17). Future structural studies of the fully liganded IDI-2, harboring both reduced coenzyme (or a coenzyme analogue) and a substrate (or inhibitor) molecule, will be helpful to verify these potential acid/base mechanisms and to identify other candidates for active site acid/base groups.

In conclusion, the work presented here represents a significant advancement toward our understanding of the catalytic mechanism of IDI-2, a flavoenzyme that has not been found in human tissues but is a critical component of the isoprenoid biosynthetic machinery of certain pathogens, including *S. aureus*. Although the catalytic role of the flavin coenzyme in IDI-2 remains elusive, the current data verify the catalytic competence of a neutral FMN_{red} that accumulates in the steady state and suggests that this species may employ acid/base chemistry to catalyze a reaction with no net redox change. Experiments designed to further explore the direct involvement of the flavin in IDI-2 chemistry are in progress. The

mechanistic insight gained from this study illustrates the chemical versatility of the flavin coenzyme, and IDI-2 serves as an interesting model for studying the chemistry and energetics of flavoenzyme catalyzed reactions.

Acknowledgments

The authors thank Prof. Kevin Dalby at the University of Texas at Austin for the use of his rapid chemical quench-flow apparatus and Prof. Ah-lim Tsai at the University of Texas Medical School, Houston, for the use of his EPR facilities and for his assistance in acquiring the EPR data. They also thank Steve Sorey at the NMR core facility at the Department of Chemistry and Biochemistry at the University of Texas for his help and expertise in conducting the in situ ^{1}H NMR assays.

REFERENCES

1. Qureshi, N.; Porter, JW. Conversion of acetyl-coenzyme A to isopentenyl pyrophosphate. In: Porter, JW.; Spurgeon, SL., editors. Biosynthesis of Isoprenoid Compounds. New York: Wiley; 1981. p. 47-94.
2. Koyama, T.; Ogura, K. Isopentenyl diphosphate isomerase and prenyltransferases. In: Cane, DE., editor. Comprehensive Natural Products Chemistry. Amsterdam: Elsevier; 1999. p. 69-96.
3. Kellogg BA, Poulter CD. Chain elongation in the isoprenoid biosynthetic pathway. Curr. Opin. Chem. Biol. 1997; 1:570–578. [PubMed: 9667899]
4. Rohdich F, Bacher A, Eisenreich W. Perspectives in anti-infective drug design. The late steps in the biosynthesis of the universal terpenoid precursors, isopentenyl diphosphate and dimethylallyl diphosphate. Bioorg. Chem. 2004; 32:292–308. [PubMed: 15381396]
5. Kuzuyama T. Mevalonate and nonmevalonate pathways for the biosynthesis of isoprene units. Biosci. Biotechnol. Biochem. 2002; 66:1619–1627. [PubMed: 12353619]
6. Rohmer M. Mevalonate-independent methylerythiyol phosphate pathway for isoprenoid biosynthesis. Elucidation and distribution. Pure Appl. Chem. 2003; 75:375–387.
7. Rohdich F, Hecht S, Bacher A, Eisenreich W. Deoxyxylulose phosphate pathway of isoprenoid biosynthesis. Discovery and function of *ispDEFGH* genes and their cognate enzymes. Pure Appl. Chem. 2003; 75:393–405.
8. Reardon JE, Abeles RH. Mechanism of action of isopentenyl pyrophosphate isomerase: Evidence for a carbonium ion intermediate. Biochemistry. 1986; 25:5609–5616. [PubMed: 3022798]
9. Muehlbacher M, Poulter CD. Isopentenyl-diphosphate isomerase: Inactivation of the enzyme with active-site-directed irreversible inhibitors and transition state analogues. Biochemistry. 1988; 27:7315–7328. [PubMed: 3207678]
10. Street IP, Christensen DJ, Poulter CD. Hydrogen exchange during the enzyme-catalyzed isomerization of isopentenyl diphosphate and dimethylallyl diphosphate. J. Am. Chem. Soc. 1990; 112:8577–8578.
11. Ramos-Valdiva AC, van der Heijden R, Verpoorte R. Isopentenyl diphosphate isomerase: A core enzyme in isoprenoid biosynthesis. A review of its biochemistry and function. Nat. Prod. Rep. 1997; 14:591–603. [PubMed: 9418296]
12. Lee S, Poulter CD. *Escherichia coli* type I isopentenyl diphosphate isomerase: Structural and catalytic roles for divalent metals. J. Am. Chem. Soc. 2006; 128:11545–11550. [PubMed: 16939278]
13. Kaneda K, Kuzuyama T, Takagi M, Hayakawa Y, Seto H. An unusual isopentenyl diphosphate isomerase in the mevalonate pathway gene cluster from *Streptomyces* sp. strain CL190. Proc. Natl. Acad. Sci. U.S.A. 2001; 98:932–937. [PubMed: 11158573]
14. Kuzuyama T, Seto H. Diversity of the biosynthesis of the isoprene units. Nat. Prod. Rep. 2003; 20:171–183. [PubMed: 12735695]
15. Laupitz R, Hecht S, Amslinger S, Zepeck F, Kaiser J, Richter G, Schramek N, Steinbacher S, Huber R, Arigoni D, Bacher A, Eisenreich W, Rohdich F. Biochemical characterization of *Bacillus subtilis* type II isopentenyl diphosphate isomerase and phylogenetic distribution of isoprenoid biosynthesis pathways. Eur. J. Biochem. 2004; 271:2658–2669. [PubMed: 15206931]

16. Steinbacher S, Kaiser J, Gerhardt S, Eisenreich W, Huber R, Bacher A, Rohdich F. Crystal structure of the type II isopentenyl diphosphate/dimethylallyl diphosphate isomerase from *Bacillus subtilis*. J. Mol. Biol. 2003; 329:973–982. [PubMed: 12798687]

17. de Ruyck J, Rothman S, Poulter CD, Wouters J. Structure of *Thermus thermophilus* type 2 isopentenyl diphosphate isomerase inferred from crystallography and molecular dynamics. Biochem. Biophys. Res. Commun. 2005; 338:1515–1518. [PubMed: 16269131]

18. Yamashita S, Hemmi H, Ikeda Y, Nakayama T, Nishino T. Type 2 isopentenyl diphosphate isomerase from a thermoacidophilic archaeon *Sulfolobus shibatae*. Eur. J. Biochem. 2004; 271:1087–1093. [PubMed: 15009187]

19. Hemmi H, Ikeda Y, Yamashita S, Nakayama T, Nishino T. Catalytic mechanism of type 2 isopentenyl diphosphate/dimethylallyl diphosphate isomerase: Verification of a redox role of the flavin cofactor in a reaction with no net redox change. Biochem. Biophys. Res. Commun. 2004; 322:905–910. [PubMed: 15336549]

20. Siddiqui MA, Yamanaka A, Hirooka K, Bamaba T, Kobayashi T, Imanaka T, Fukusaki E-i, Fujiwara S. Enzymatic and structural characterization of type II isopentenyl diphosphate isomerase from hyperthermophilic archaeon *Thermococcus kodakaraensis*. Biochem. Biophys. Res. Commun. 2005; 331:1127–1136. [PubMed: 15882994]

21. Kittleman W, Thibodeaux CJ, Zhang H, Liu Y-n, Liu H-w. Characterization and mechanistic studies of type II isopentenyl diphosphate/dimethylallyl diphosphate isomerase from *Staphylococcus aureus*. Biochemistry. 2007; 46:8401–8413. [PubMed: 17585782]

22. Rothman S, Helm TR, Poulter CD. Kinetic and spectroscopic characterization of type II isopentenyl diphosphate isomerase from *Thermus thermophilus*: Evidence for the formation of substrate-induced flavin species. Biochemistry. 2007; 46:5437–5445. [PubMed: 17428035]

23. Bornemann S. Flavoenzymes that catalyze reactions with no net redox change. Nat. Prod. Rep. 2002; 19:761–772. [PubMed: 12521268] Ibid. Med. Chem. 14:6555–6559.

24. Johnston JB, Walker JR, Rothman SC, Poulter CD. Type 2 isopentenyl diphosphate isomerase. Mechanistic studies with cyclopropyl and epoxy analogues. J. Am. Chem. Soc. 2007; 129:7740–7741. [PubMed: 17547410]

25. Hoshino T, Tamegai H, Kakinuma K, Eguchi T. Inhibition of type 2 isopentenyl diphosphate isomerase from *Methanocaldococcus jannaschii* by a mechanism-based inhibitor of type 1 isopentenyl diphosphate isomerase. Bioorg. Med. Chem. 2006; 14:6555–6559. [PubMed: 16793276]

26. Bradford MM. A rapid and sensitive method for the quantitation of microgram quantities of protein utilizing the principle of protein–dye binding. Anal. Biochem. 1976; 72:248–254. [PubMed: 942051]

27. Davisson VJ, Woodside AB, Poulter CD. Synthesis of allylic and homoallylic isoprenoid pyrophosphates. Methods Enzymol. 1985; 110:130–144. [PubMed: 2991702]

28. Kao, C-l; Kittleman, W.; Zhang, H.; Seto, H.; Liu, H-w. Stereochemical analysis of isopentenyl diphosphate isomerase type II from *Staphylococcus aureus* using chemically synthesized (*S*)- and (*R*)-[2-^{2}H]isopentenyl diphosphates. Org. Lett. 2005; 7:5677–5680. [PubMed: 16321020]

29. Hersh LB, Walsh C. Preparation, characterization, and coenzymic properties of 5-carba-5-deaza and 1-carba-1-deaza analogues of riboflavin, FMN, and FAD. Methods Enzymol. 1980; 66:277–287. [PubMed: 6246390]

30. Muller, F. Free flavins: Syntheses, chemical and physical properties. In: Muller, F., editor. Chemistry and Biochemistry of Flavoenzymes. Boca Raton, FL: CRC Press, Inc.; 1991. p. 1-72.

31. Mansoorabadi SO, Thibodeaux CJ, Liu H-w. The diverse roles of flavin coenzymes: Nature's most versatile thespians. J. Org. Chem. 2007; 72:6329–6342. [PubMed: 17580897]

32. Ghisla S, Massey V, Lhoste J-M, Mayhew SG. Fluorescence and optical characteristics of reduced flavines and flavoproteins. Biochemistry. 1974; 13:589–597. [PubMed: 4149231]

33. Macheroux P, Bornemann S, Ghisla S, Thorneley RNF. Studies with flavin analogues provide evidence that a protonated reduced FMN is the substrate-induced transient intermediate in the reaction of *Escherichia coli* chorismate synthase. J. Biol. Chem. 1996; 271:25850–25858. [PubMed: 8824216]

34. Corrado ME, Aliverti A, Zanetti G, Meyhew SG. Analysis of the oxidation–reduction potentials of recombinant ferredoxin-$NADP^+$ reductase from spinach chloroplasts. Eur. J. Biochem. 1996; 239:662–667. [PubMed: 8774710]
35. Yalloway GN, Mayhew SG, Malthouse JPG, Gallagher ME, Curley GP. pH-dependent spectroscopic changes associated with the hydroquinone of FMN in flavodoxins. Biochemistry. 1999; 38:3753–3762. [PubMed: 10090764]
36. Spencer R, Fisher J, Walsh C. Preparation, characterization, and chemical properties of the flavin coenzyme analogues 5-deazariboflavin, 5-deazariboflavin 5′-phosphate, and 5-deazariboflavin 5′-diphosphate and 5′-5′-adenosine ester. Biochemistry. 1976; 15:1043–1053. [PubMed: 3206]
37. Spencer R, Fisher J, Walsh C. One- and two-electron redox chemistry of 1-carba-1-deaza-riboflavin. Biochemistry. 1977; 16:3586–3594. [PubMed: 19057]
38. Walsh, C.; Fisher, J.; Jacobson, F.; Spencer, R.; Ashton, W.; Brown, R. Coenzymic properties of flavin analogues, in *Flavins and Flavoproteins*. In: Yagi, K.; Yamano, T., editors. Proceedings of the 6th International Symposium (1980); Japan Science Society Press; Tokyo, Japan. 1978. p. 13-21.
39. Kay, CMW.; Weber, S. EPR of radical intermediates in flavoenzymes. In: Gilbert, BC.; Davies, MJ.; Murphy, DM., editors. Electron Paramagnetic Resonance. London: Royal Society of Chemistry; 2002. p. 222-253.
40. Toteva MM, Richard JP. Mechanistic imperatives for the reaction catalyzed by isopentenyl pyrophosphate isomerase: Free energy profile for stepwise isomerization in water through a tertiary carbocation intermediate. Bioorg. Chem. 1997; 25:239–245.
41. Ghisla S, Massey V. New flavins for old: Artificial flavins as active site probes of flavoproteins. Biochem. J. 1986; 239:1–12. [PubMed: 3541919]
42. Ghisla, S.; Macheroux, P.; Sanner, C.; Rueterjans, H.; Mueller, F. Ionization properties or reduced, 1,5-dihydroflavin, rates of N(5)-H exchange with solvent. In: Curti, B.; Ronchi, S.; Zanetti, G., editors. Flavins and Flavoproteins, Proceedings of the 10th International Symp., 10th (1991); de Gruyter; Berlin. 1990. p. 27-32.
43. Macheroux P, Ghisla S, Sanner C, Rueterjans H, Muller F. Reduced flavin: NMR investigation of N(5)-H exchange mechanism, estimation of ionisation constants and assessment of properties as biological catalyst. BMC Biochem. 2005; 6:1–11. [PubMed: 15715904]
44. Ghisla S, Thorpe C. Acyl-CoA dehydrogenases. Eur. J. Biochem. 2004; 271:494–508. [PubMed: 14728676]

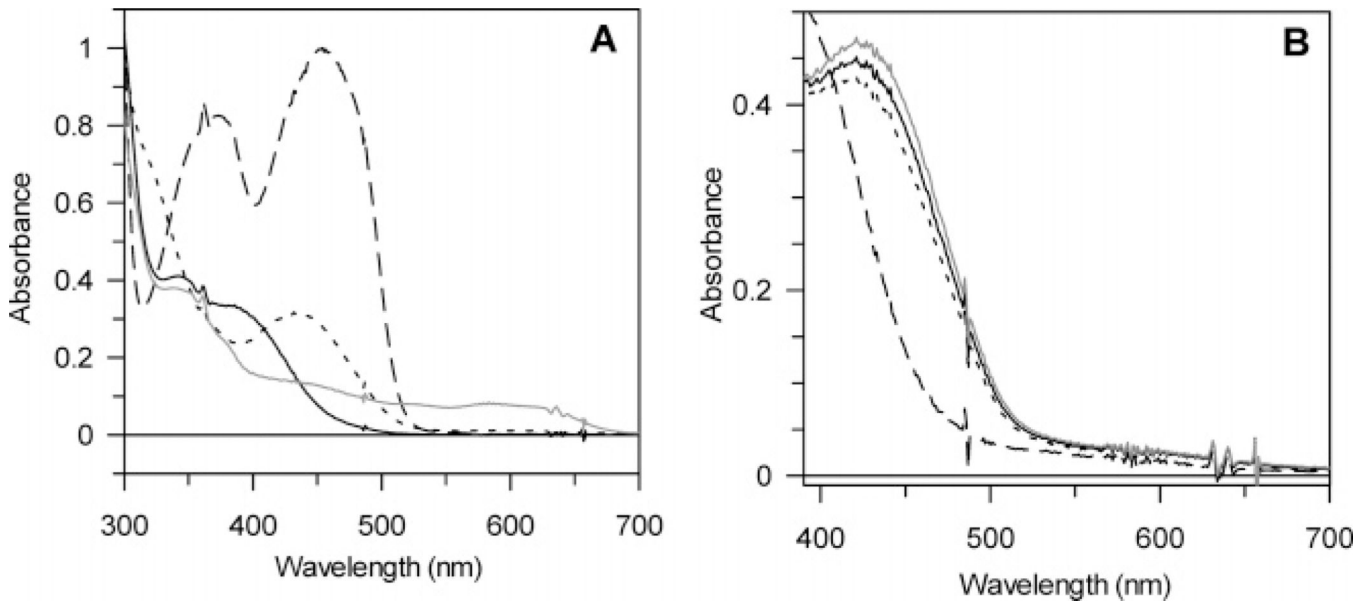

FIGURE 1.

UV–vis spectra of various forms of the IDI-2-bound FMN. Reaction conditions are given in the Experimental Procedures. (A) An 80 μM solution of E•FMN_{ox} (dashed line) was photoreduced under anaerobic conditons to give E•FMN_{red} (solid black line). Addition of 2 mM IPP led to the intermediate spectrum (dotted line). If 2 mM IPP was pre-incubated with E•FMN_{ox} prior to photoreduction, the neutral semiquinone is formed (solid gray line). (B) Spectra of dithionite (10 mM) reduced E•FMN_{red} (80 μM, dashed line) and the flavin intermediates formed upon addition of 2 mM IPP (solid black line), (*R*)-[2-^{2}H]-IPP (solid gray line), or DMAPP (dotted line).

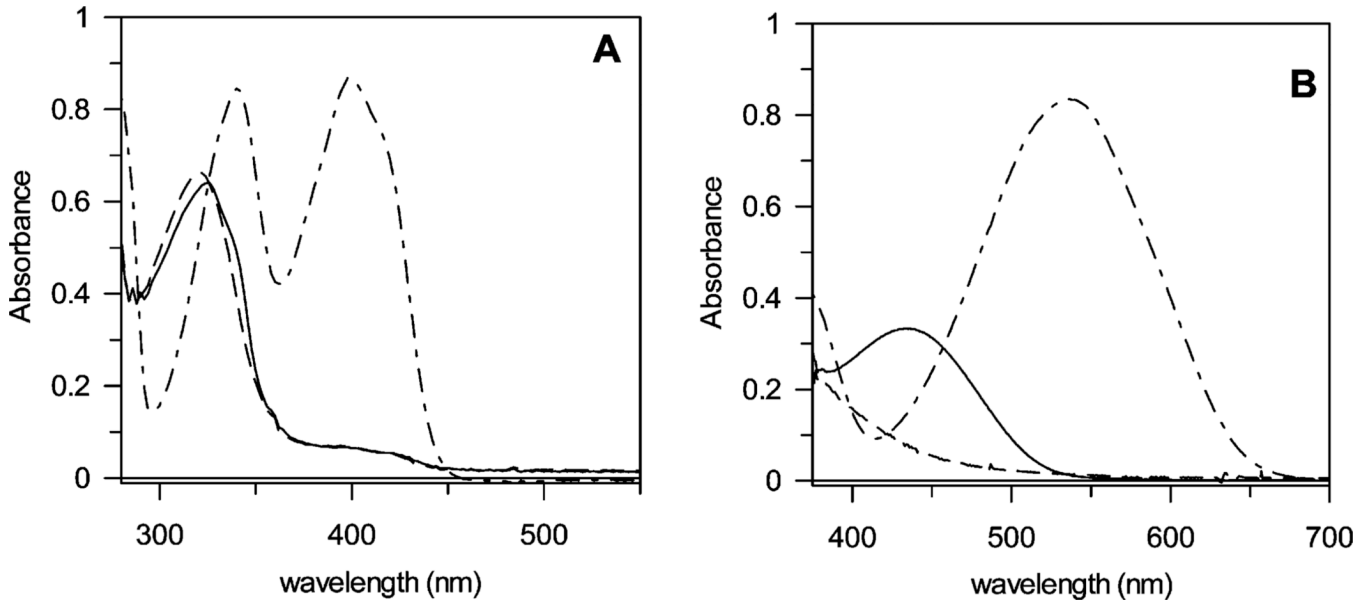

FIGURE 2.

UV–vis absorbance spectra of the oxidized (-•-•-) and reduced (----) forms of enzyme-bound 5-deazaFMN (A) and 1-deazaFMN (B) bound to IDI-2 at pH 7.0 and 25 °C. E•5-deazaFMN$_{ox}$ was photoreduced, while E•1-deazaFMN$_{ox}$ required chemical reduction with sodium dithionite (see Experimental Procedures for details). When 1 mM IPP was added to the reduced enzymes, a unique flavin species (—) formed. The spectra of these species are consistent with the neutral reduced coenzymes.

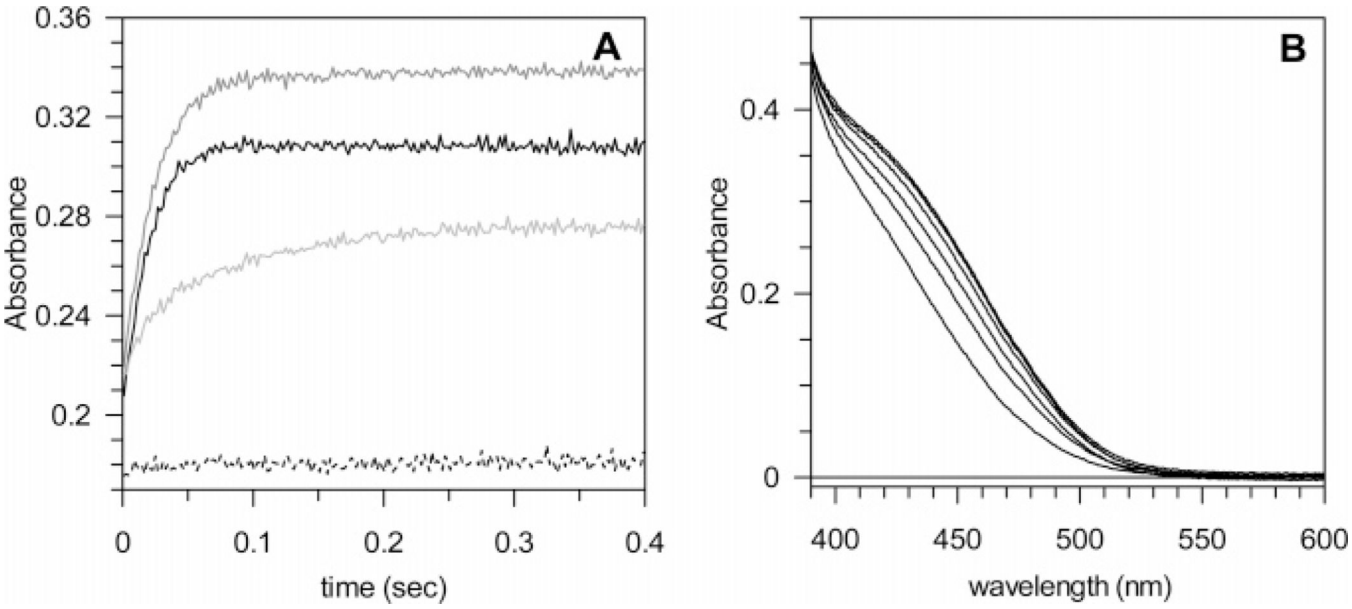

FIGURE 3.

Stopped-flow spectrophotometry of flaivn intermediate formation. (A) Pre-steady-state changes in A_{435} recorded over 400 ms for the reaction of 68 μM E•FMN_{red} with 2 mM IPP (black line), 2 mM DMAPP (light gray line), and 2 mM (*R*)-[2-^{2}H]-IPP (dark gray line). When enzyme was mixed against buffer, there was no change in A_{435} (dotted line). The time courses at 435 nm were fit to a single-exponential equation (eq 1) to determine the amplitude of the absorbance change (*A*), the observed rate (k_{obs}), and the initial A_{435} (*C*). For IPP: $A = 0.11 \pm 0.001$ AU (absorbance units); $k_{obs} = 52 \pm 0.9$ s^{-1}; and $C = 0.20 \pm 0.001$ AU. For DMAPP: $A = 0.053 \pm 0.0007$ AU; $k_{obs} = 14.8 \pm 0.4$ s^{-1}; and $C = 0.223 \pm 0.0008$ AU. For (*R*)-[2-^{2}H]-IPP: $A = 0.12 \pm 0.001$; $k_{obs} = 40.9 \pm 0.5$ s^{-1}; and $C = 0.21 \pm 0.001$ AU. (B) Pre-steady state accumulation of the flavin intermediate in the reaction of 68 μM E•FMN_{red} (reduced with 10 mM dithionite) with 2 mM IPP. Spectra from bottom to top at 435 nm were obtained 0.001, 0.013, 0.025, 0.037, 0.075, and 0.399 s after mixing.

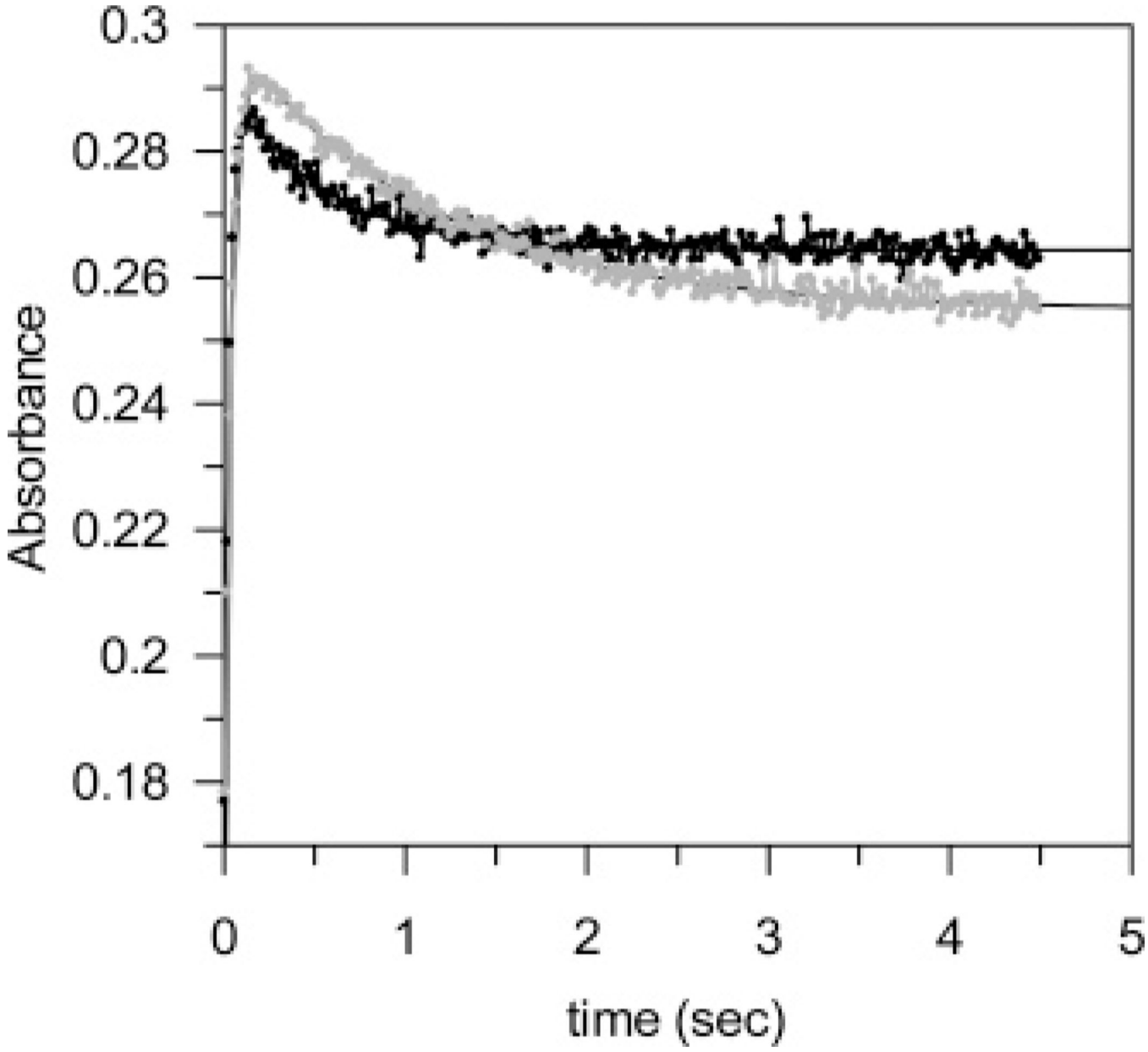

FIGURE 4.

Single-turnover kinetics of flavin intermediate formation and decay over 5 s. IDI-2 was mixed in a molar excess over either IPP (black) or (*R*)-[2-^{2}H]-IPP (gray), and the formation and decay of the flavin intermediate was followed at 435 nm. The time courses were fit to double-exponential equations to extract the amplitudes and the observed rates for the fast (increasing A_{435}) and slow (decreasing A_{435}) phases. Eight injections were performed with each substrate, and the average rates and amplitudes were determined. For IPP: $A_f = 0.14 \pm 0.01$ AU, $k_f = 34 \pm 2.4$ s^{-1}, $A_s = -0.028 \pm 0.009$ AU, and $k_s = 2.1 \pm 0.4$ s^{-1}. For (*R*)-[2-^{2}H]-IPP: $A_f = 0.14 \pm 0.007$ AU, $k_f = 23 \pm 0.9$ s^{-1}, $A_s = -0.043 \pm 0.001$ AU, and $k_s = 0.9 \pm 0.05$ s^{-1}.

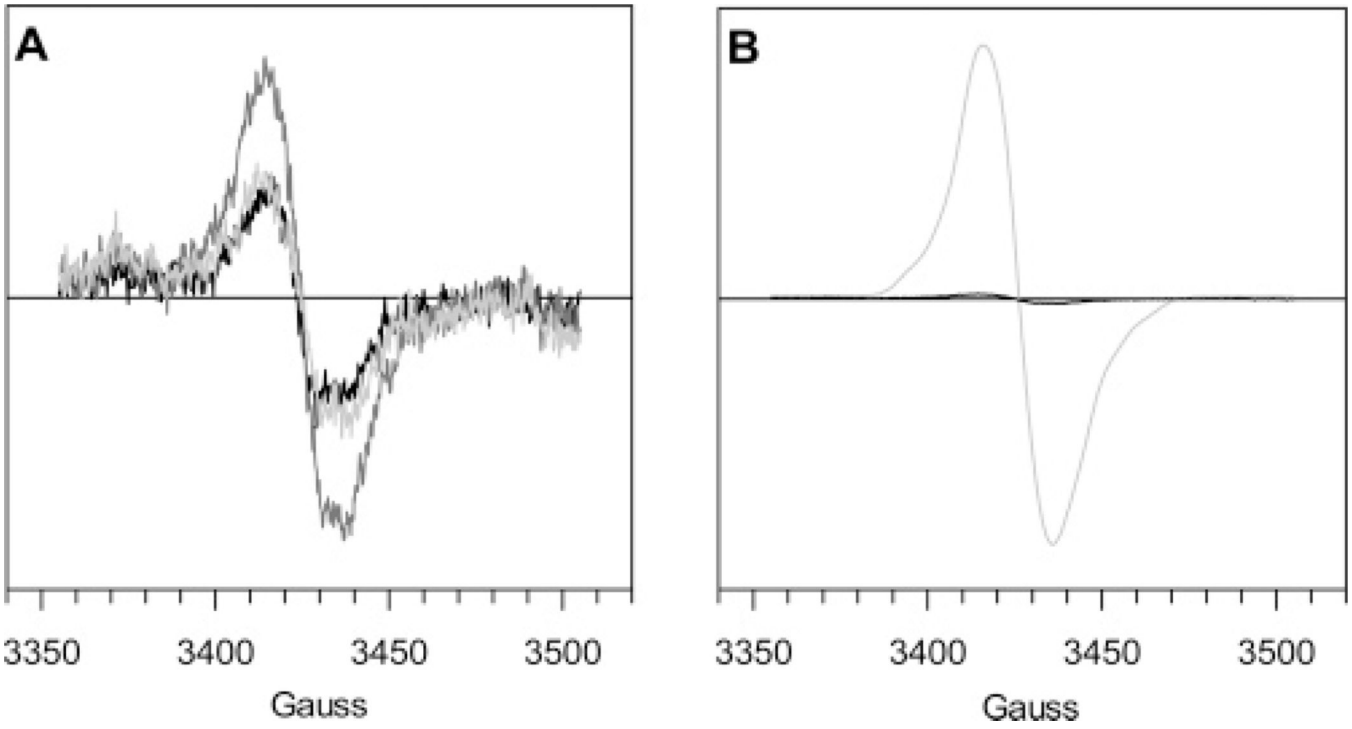

FIGURE 5.

X-band EPR spectra recorded for reaction mixtures containing 80 μM IDI-2, 200 μM FMN, and 2 mM IPP. The FMN coenzyme was either photoreduced (A, light gray) or chemically reduced by 10 mM dithionite (A, black) or 10 mM NADPH (A, dark gray) prior to the addition of 2 mM IPP. After 2 min, the reactions were flash frozen and stored in liquid nitrogen until the spectra were recorded. The concentration of FMN_{sem} was determined to be 0.39, 0.86, and 0.72 μM for dithionite reduced, NADPH reduced, and photoreduced samples, respectively. These values correspond to 0.5, 1, and 0.9% of the total enzyme concentration. (B) In contrast to these reaction mixtures, the photoreduced E•FMN_{ox}•IPP mixture (gray) yielded 29.6 μM neutral semiquinone, corresponding to 37% of the total enzyme concentration. The spectrum of the NADPH reduced reaction mixture (black) is shown for comparison. Experimental conditions: temperature, 100 K; modulation amplitude, 5 G; microwave power, 1 mW; and spectrometer frequency, 9.601 GHz. The spectra are an average of five 3 min scans.

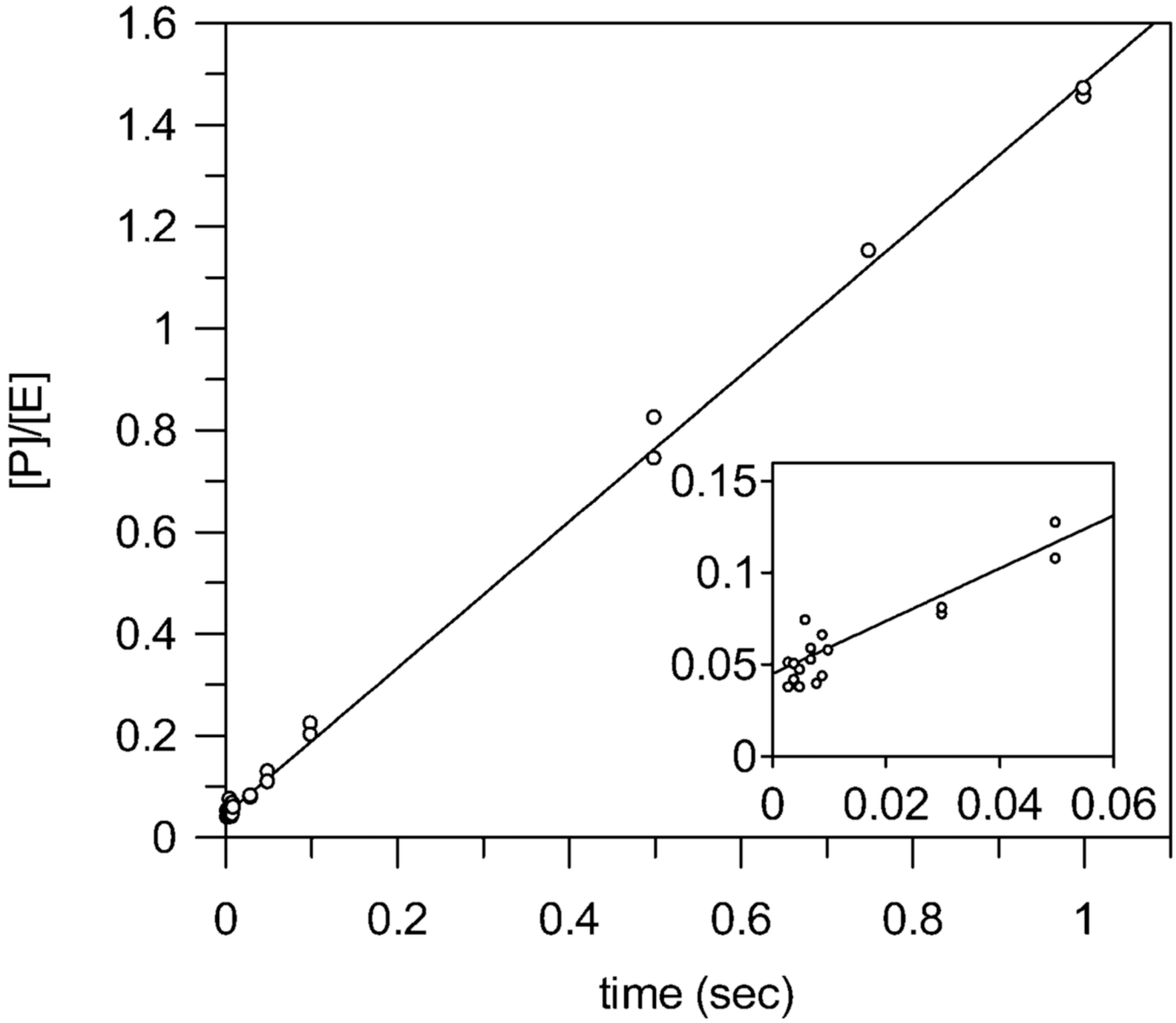

FIGURE 6.

Pre-steady-state formation of DMAPP in the rapid-mix chemical quench experiment. The reaction contained 19.7 μM IDI-2, 100 μM FMN, 100 mM dithionite, and 520 μM IPP in 100 mM HEPES, 5 mM $MgCl_2$, and 1 mM DTT (pH 7.0 and 37 °C). Both enzyme and IPP solutions contained all of the other reaction components. Individual injections were quenched at varying times (0.003, 0.004, 0.005, 0.006, 0.007, 0.008, 0.009, 0.010, 0.030, 0.050, 0.100, 0.500, 0.750, and 1.000 s) by 25% HCl/MeOH after mixing IDI-2 and [1-^{14}C]-IPP (specific activity = 1.92 μCi/μmol). The workup and extraction procedures to detect DMAPP are described in the Experimental Procedures. The concentration of DMAPP at each time point was calculated and normalized by the total enzyme concentration. The data fit a line with a slope of 1.4 ± 0.01 s^{-1} and a *y*-intercept of 0.04 ± 0.01. The inset shows a closer view of the early time points.

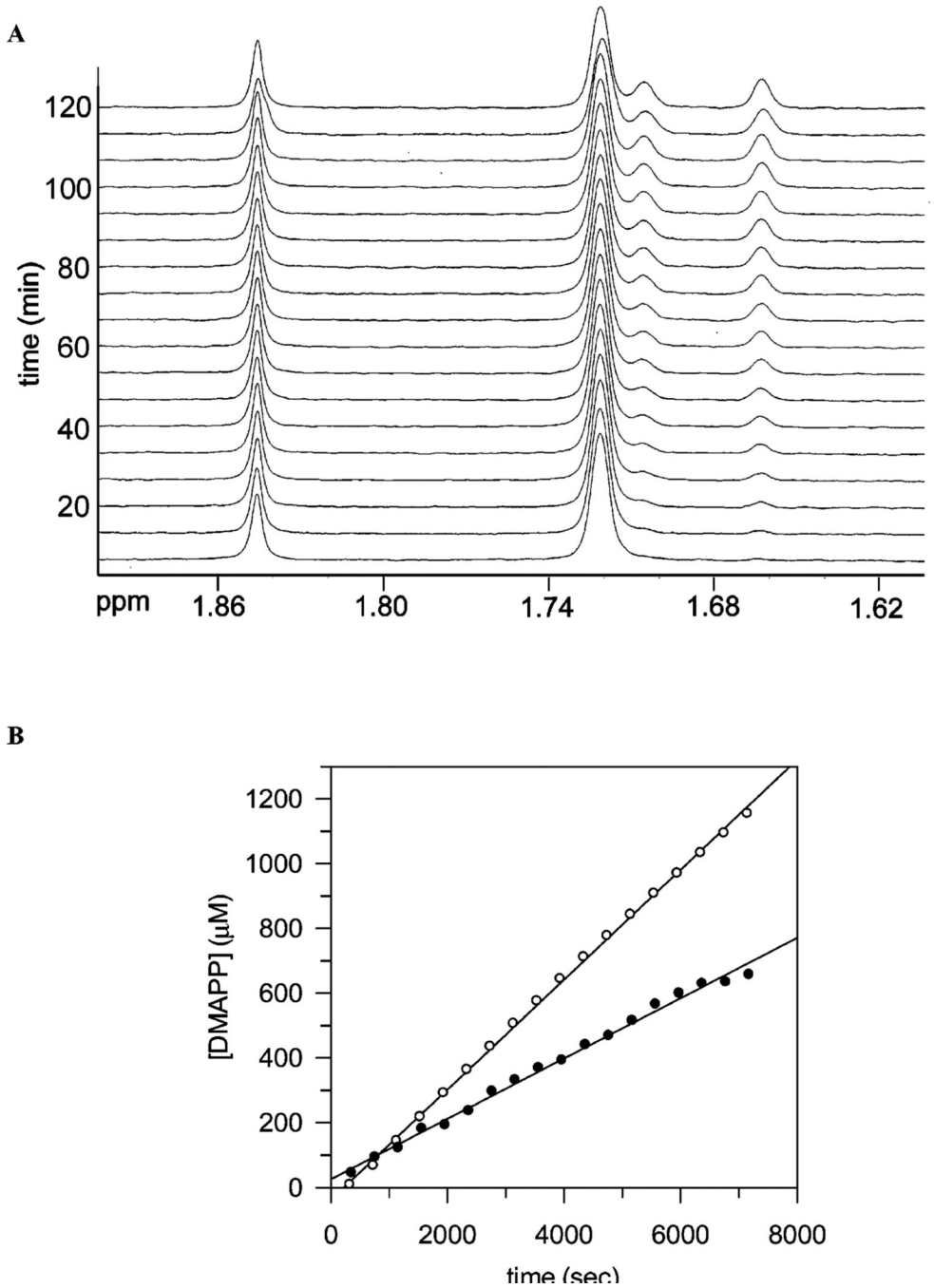

FIGURE 7.

Substrate deuterium KIE on V_{max}. (A) ^{1}H NMR assay showing the conversion of IPP (C4′ methyl singlet at δ = 1.72 ppm) to DMAPP ((*E*)-methyl singlet at δ = 1.70 ppm and (*Z*)-methyl singlet at δ = 1.66 ppm). (B) Plot showing the formation of DMAPP from IPP (white circles) and (*R*)-[2-^{2}H]-IPP (black circles) as a function of time. The integrated (*Z*)-methyl peak areas of DMAPP were normalized by the 2 mM acetate signal (δ = 1.84 ppm) to calculate the concentration of DMAPP at each time point. The initial velocities were determined from these plots to be 0.170 ± 0.001 μM s^{-1} for IPP and 0.093 ± 0.002 μM s^{-1} for (*R*)-[2-^{2}H]-IPP, yielding $^{D}V_{max}$ = 1.8 ± 0.04.

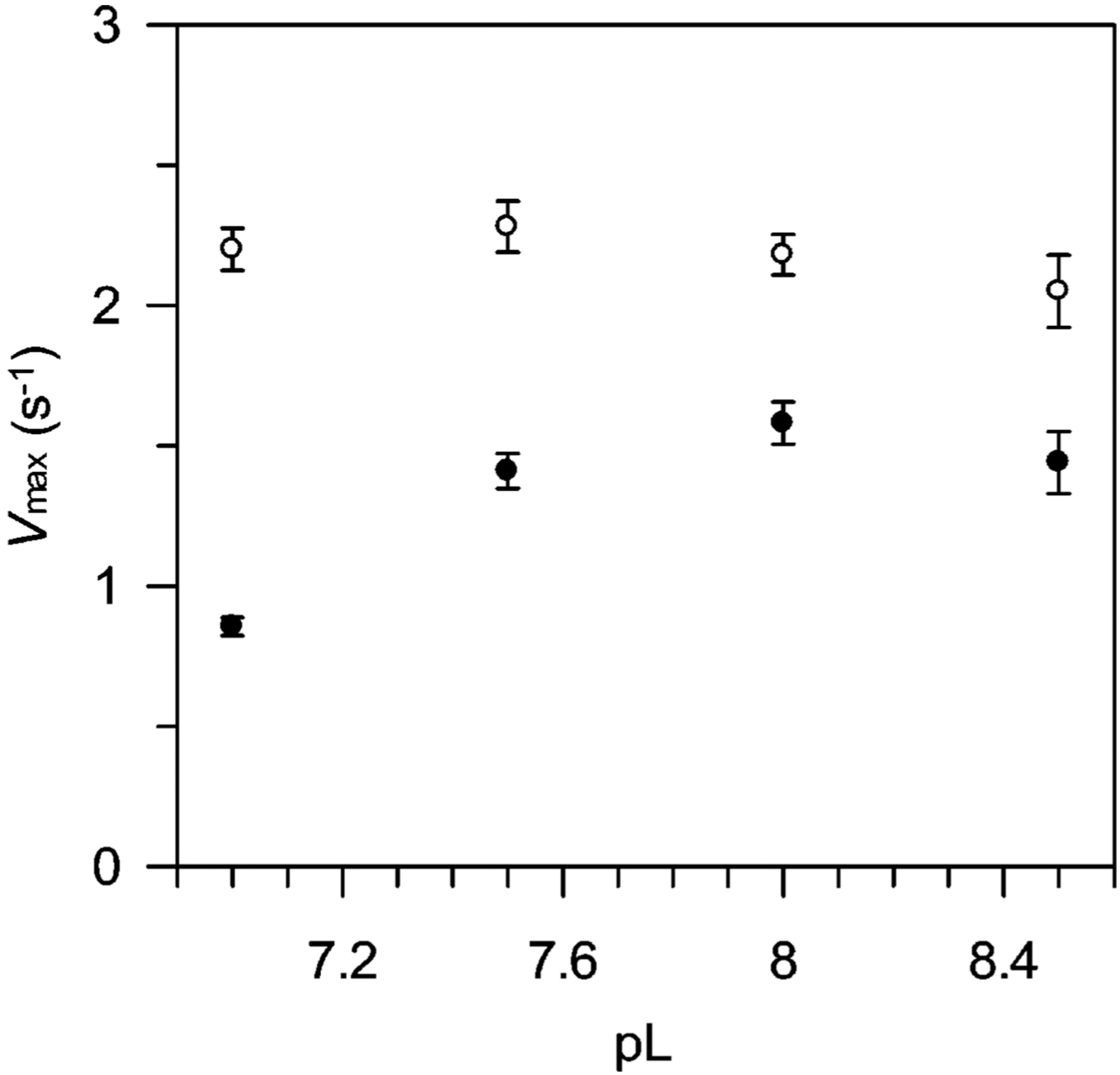

FIGURE 8.

Solvent kinetic isotope effects on V_{max}. The initial velocity (v_o) of DMAPP formation at 269 μM IPP was determined in triplicate under anaerobic conditions at pL 7.0, 7.5, 8.0, and 8.5. The velocities in H_2O (white circles) were consistently higher than the velocities in D_2O (black circles). The corrected $^{D_2O}V_{max}$ was calculated to be 1.4 ± 0.08 at pL 8.0 (see Experimental Procedures). The $^{D_2O}V_{max}$ at pL 8.0 was taken to be the most accurate value because this range appears to be the pL-independent region of v_o for both solvents.

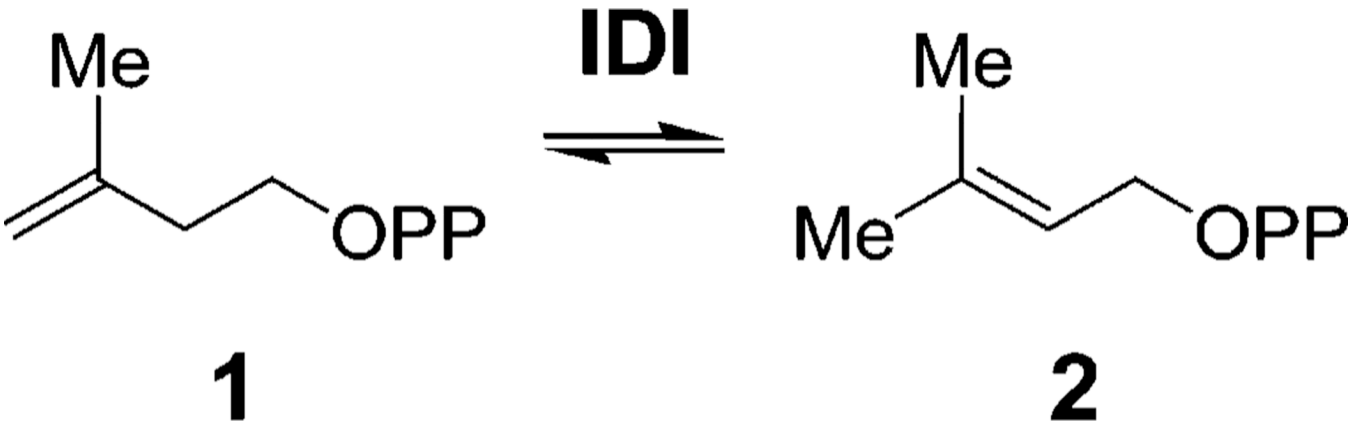

Scheme 1.

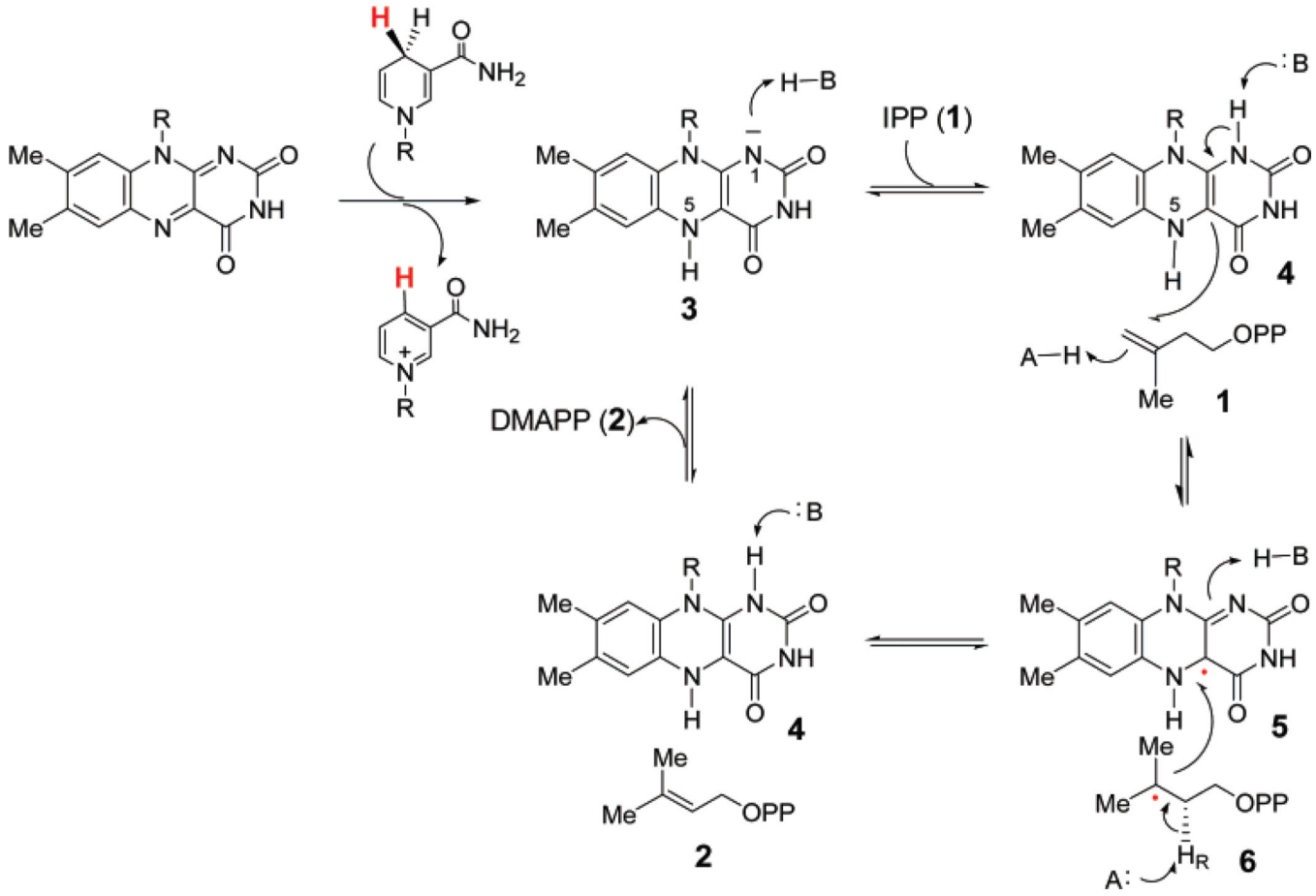

Scheme 2.

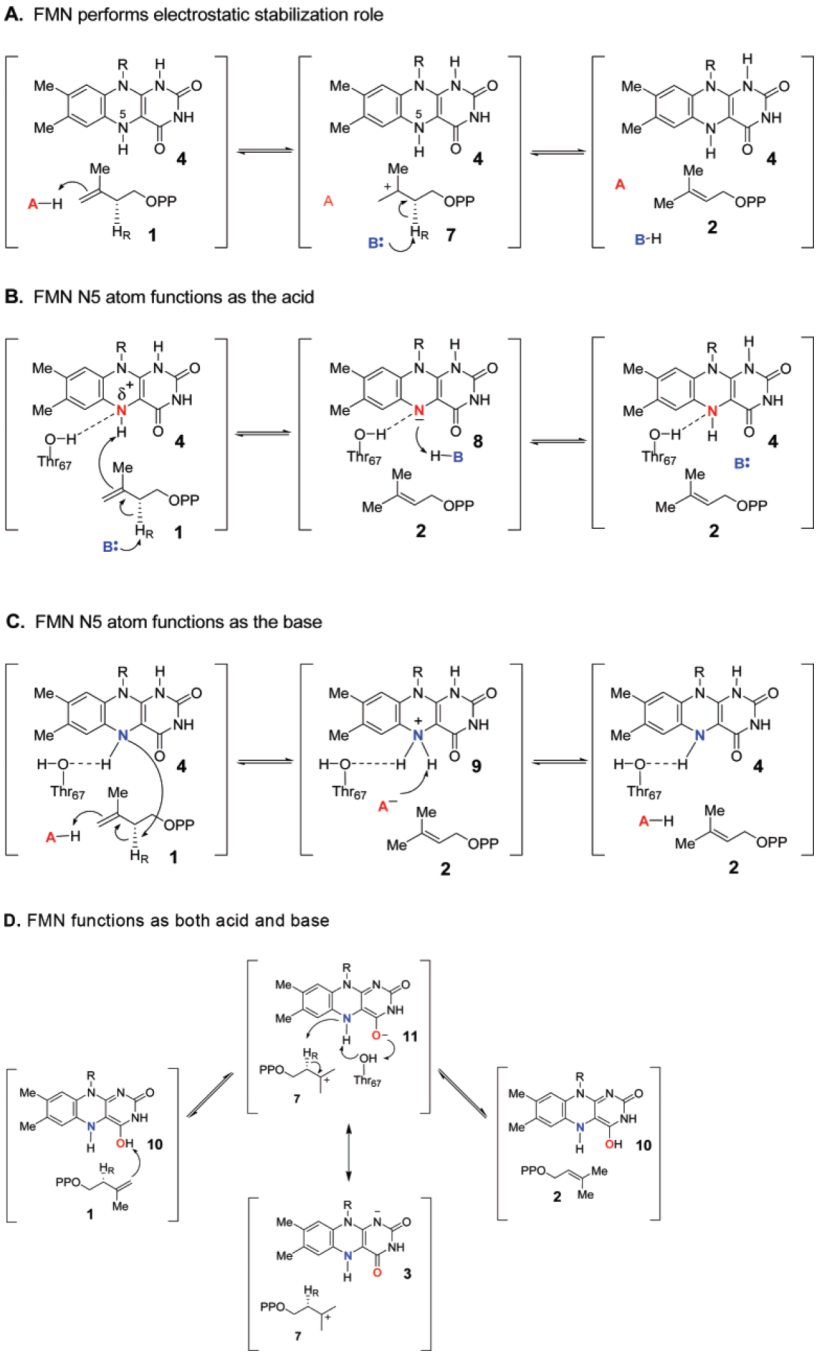

Scheme 3.